

Supporting information:  
Protonation and water exchange kinetics in sandwich  
polyoxometalates.

C. André Ohlin<sup>1</sup>

<sup>1</sup>Department of Chemistry, Umeå University, Sweden

*Department of Chemistry, Umeå University, Sweden*

## Contents

### List of Tables

S1	Energies, bond distances and partial charges using different partition methods in $\text{H}_2[\text{Zn}_4(\text{H}_2\text{O})_2(\text{PW}_9\text{O}_{34})_2]^{8-}$ as a function of protonation site. Geometries optimised at pbe0/def2-svp with PCM. The $d(\text{M}-\text{OH}_2)$ in the non-protonated form is 2.192 Å. Partial charges were calculated for the unprotonated molecule. . . . .	4
S2	Energies and bond distances in $\text{H}_2[\text{Zn}_4(\text{H}_2\text{O})_2(\text{PW}_9\text{O}_{34})_2]^{8-}$ (left) and $\text{H}_4[\text{Zn}_4(\text{H}_2\text{O})_2(\text{PW}_9\text{O}_{34})_2]^{6-}$ (right) as a function of protonation site. Geometries optimised at pbe0/def-svp with PCM. The $d(\text{M}-\text{OH}_2)$ in the non-protonated form is 2.192 Å. . . . .	4
S3	Energies and bond distances in $\text{H}_2[\text{Zn}_4(\text{H}_2\text{O})_2(\text{PW}_9\text{O}_{34})_2]^{8-}$ (left) and $\text{H}_4[\text{Zn}_4(\text{H}_2\text{O})_2(\text{PW}_9\text{O}_{34})_2]^{6-}$ (right) as a function of protonation site. Geometries optimised at pbe0/def2-tzvp with PCM. The $d(\text{M}-\text{OH}_2)$ in the non-protonated form is 2.236 Å. . . . .	5
S4	Bond parameters obtained from crystal structures, and rates of aquo-ligand exchange. Average bond distances were used where there were several different types of water ligands. . . . .	6

### List of Figures

S1	Structure of $[\text{Zn}_4(\text{H}_2\text{O})_2(\text{PW}_9\text{O}_{34})_2]^{10-}$ . $\mu_2$ -O sites are labelled A-J and L, the single $\mu_3$ -O site is labelled K, and the terminal $\eta$ -O sites are labelled N-Q. . . . .	3
S2	Top: Zn-OH <sub>2</sub> distance as a function of basis set. Bottom: $r$ vs protonation site, where $r$ is the Zn-OH <sub>2</sub> distance as a function of basis set divided by the Zn-OH <sub>2</sub> distance in the unprotonated complex at the same level of theory. Def2-svp results given as red squares and def2-tzvp data given as empty blue circles. The larger basis set gives longer absolute Zn-OH <sub>2</sub> distances, but also predicts a larger contraction due to protonation. . . . .	7
S3	Comparison of partial charges from different methods at pbe0/def2-svp with relative energies of $\text{H}_2[\text{Zn}_4(\text{H}_2\text{O})_2(\text{PW}_9\text{O}_{34})_2]^{8-}$ protonated in different loci. All partial charges methods indicate that site K ( $\mu_3$ ) has the most negative partial charge. . . . .	8

### Listings

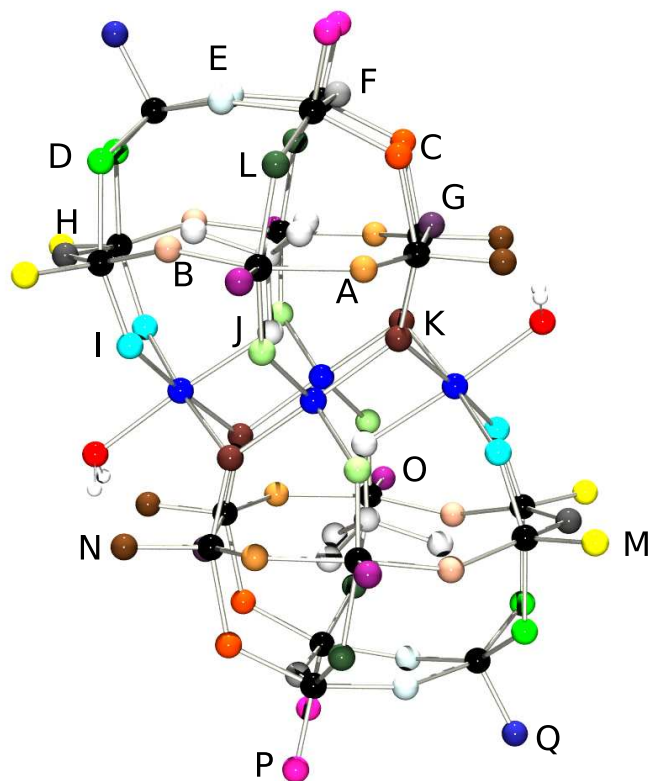


Figure S1: Structure of  $[\text{Zn}_4(\text{H}_2\text{O})_2(\text{PW}_9\text{O}_{34})_2]^{10-}$ .  $\mu_2$ -O sites are labelled A-J and L, the single  $\mu_3$ -O site is labelled K, and the terminal  $\eta$ -O sites are labelled N-Q.

Table S1: Energies, bond distances and partial charges using different partition methods in  $\text{H}_2[\text{Zn}_4(\text{H}_2\text{O})_2(\text{PW}_9\text{O}_{34})_2]^{8-}$  as a function of protonation site. Geometries optimised at pbe0/def2-svp with PCM. The  $d(\text{M}-\text{OH}_2)$  in the non-protonated form is 2.192 Å. Partial charges were calculated for the unprotonated molecule.

Entry	Site	$\epsilon$ (Hartree)	$\Delta\epsilon$ (kcal/mol)	$d(\text{M}-\text{OH}_2)$ (Å)	NBO <sup>a</sup> (a.u.)	MKUFF <sup>b</sup> (a.u.)	CHelpG <sup>c</sup> (a.u.)	HLYGAt <sup>d</sup> (a.u.)
1	A ( $\mu_2$ )	-14271.4963027	23.026	2.171	-0.9212	-0.8996	-0.8946	-0.7597
2	B ( $\mu_2$ )	-14271.5005239	20.378	2.166	-0.9379	-0.9492	-0.9098	-0.7476
3	C ( $\mu_2$ )	-14271.5026127	19.067	2.167	-0.9279	-0.9000	-0.8750	-0.7821
4	D ( $\mu_2$ )	-14271.5050184	17.557	2.169	-0.9355	-0.9091	-0.8667	-0.7774
5	E ( $\mu_2$ )	-14271.5088241	15.169	2.168	-0.9404	-0.9243	-0.8716	-0.7510
6	F ( $\mu_2$ )	-14271.5098391	14.532	2.162	-0.9381	-0.9236	-0.8859	-0.7524
7	G ( $\mu_2$ )	-14271.5061181	16.867	2.164	-0.9325	-0.9560	-0.8883	-0.7946
8	H ( $\mu_2$ )	-14271.5040763	18.148	2.171	-0.9344	-0.9112	-0.9134	-0.7677
9	I ( $\mu_2$ )	-14271.5322401	0.476	2.156	-0.9581	-0.9626	-0.9230	-0.8581
10	J ( $\mu_2$ )	-14271.5329979	0	2.160	-0.9614	-0.9553	-0.9477	-0.8166
11	K ( $\mu_3$ )	-14271.5104687	14.137	2.167	<i>-1.0928</i>	<i>-1.0320</i>	<i>-1.0141</i>	<i>-1.0917</i>
12	L ( $\mu_2$ )	-14271.4999138	20.760	2.162	-0.9422	-0.9318	-0.8967	-0.8009
13	M ( $\eta$ )	-14271.4608424	45.278	2.165	-0.7634	-0.7086	-0.7474	-0.6412
14	N ( $\eta$ )	-14271.4515435	51.113	2.167	-0.7908	-0.7139	-0.7506	-0.6506
15	O ( $\eta$ )	-14271.4604518	45.523	2.170	-0.7639	-0.7067	-0.7492	-0.6384
16	P ( $\eta$ )	-14271.4468487	54.059	2.175	-0.7537	-0.6858	-0.7261	-0.6226
17	Q ( $\eta$ )	-14271.4482246	53.196	2.172	-0.7561	-0.6903	-0.7211	-0.6281

<sup>a</sup> Natural atomic charges from Natural Bond Order analysis.[1] <sup>b</sup> The Mesler-Singh-Kollman scheme, using UFF radii.[2] <sup>c</sup> Breneman's modified CHelp scheme, using radii of 1.39 and 1.80 Å for Zn and W, respectively.[3] <sup>d</sup> The Hu, Lu, and Yang charge fitting method using G09 standard atom densities.[4] The most negatively charged oxygen for each method is given in italics.

Table S2: Energies and bond distances in  $\text{H}_2[\text{Zn}_4(\text{H}_2\text{O})_2(\text{PW}_9\text{O}_{34})_2]^{8-}$  (left) and  $\text{H}_4[\text{Zn}_4(\text{H}_2\text{O})_2(\text{PW}_9\text{O}_{34})_2]^{6-}$  (right) as a function of protonation site. Geometries optimised at pbe0/def-svp with PCM. The  $d(\text{M}-\text{OH}_2)$  in the non-protonated form is 2.192 Å.

Entry	Site	$(\text{H}_2[\text{Zn}_4(\text{H}_2\text{O})_2(\text{PW}_9\text{O}_{34})_2]^{8-})$			$(\text{H}_4[\text{Zn}_4(\text{H}_2\text{O})_2(\text{PW}_9\text{O}_{34})_2]^{6-})$		
		$\epsilon$ (Hartree)	$\Delta\epsilon$ (kcal/mol)	$d(\text{M}-\text{OH}_2)$ (Å)	$\epsilon$ (Hartree)	$\Delta\epsilon$ (kcal/mol)	$d(\text{M}-\text{OH}_2)$ (Å)
1	I	-14271.5322401	0.476	2.156	-14272.4578948	-0.294	2.119
2	J	-14271.5329979	0	2.160	-14272.4574264	0	2.132
3	K	-14271.5104687	14.137	2.167	-14272.4146286	26.856	2.130

$\Delta\epsilon$  given relative to the lowest energy configuration for each protonation state.

Table S3: Energies and bond distances in  $H_2[Zn_4(H_2O)_2(PW_9O_{34})_2]^{8-}$  (left) and  $H_4[Zn_4(H_2O)_2(PW_9O_{34})_2]^{6-}$  (right) as a function of protonation site. Geometries optimised at pbe0/def2-tzvp with PCM. The  $d(M-OH_2)$  in the non-protonated form is 2.236 Å.

Entry	Site	$(H_2[Zn_4(H_2O)_2(PW_9O_{34})_2]^{8-})$			$(H_4[Zn_4(H_2O)_2(PW_9O_{34})_2]^{6-})$		
		$\epsilon$ (Hartree)	$\Delta\epsilon$ (kcal/mol)	$d(M-OH_2)$ (Å)	$\epsilon$ (Hartree)	$\Delta\epsilon$ (kcal/mol)	$d(M-OH_2)$ (Å)
1	A ( $\mu_2$ )	-14279.3302237	22.038	2.207	—	—	—
2	B ( $\mu_2$ )	-14279.3322006	20.798	2.199	—	—	—
3	C ( $\mu_2$ )	-14279.3341081	19.601	2.199	—	—	—
4	D ( $\mu_2$ )	-14279.3372344	17.639	2.202	—	—	—
5	E ( $\mu_2$ )	-14279.3383597	16.933	2.200	—	—	—
6	F ( $\mu_2$ )	-14279.3391176	16.457	2.193	—	—	—
7	G ( $\mu_2$ )	-14279.3357358	18.579	2.199	—	—	—
8	H ( $\mu_2$ )	-14279.3386754	16.735	2.205	—	—	—
9	I ( $\mu_2$ )	-14279.3653335	0.007	2.183	-14280.2894352	0.200	2.138
10	J ( $\mu_2$ )	-14279.3653439	0	2.190	-14280.2897538	0	2.152
11	K ( $\mu_3$ )	-14279.3439098	13.450	2.202	-14280.2457475	27.614	2.153
12	L ( $\mu_2$ )	-14279.3321491	20.830	2.193	—	—	—
13	M ( $\eta$ )	-14279.3001521	40.908	2.197	—	—	—
14	N ( $\eta$ )	-14279.2907393	46.815	2.202	—	—	—
15	O ( $\eta$ )	-14279.2997023	41.190	2.202	—	—	—
16	P ( $\eta$ )	-14279.2845071	50.725	2.209	—	—	—
17	Q ( $\eta$ )	-14279.2861521	49.693	2.207	—	—	—

Table S4: Bond parameters obtained from crystal structures, and rates of aquo-ligand exchange. Average bond distances were used where there were several different types of water ligands.

Entry	Compound	M-O bond distance (Å) <sup>a</sup>	k (s <sup>-1</sup> )	References
1	[Ni(H <sub>2</sub> O) <sub>6</sub> ] <sup>2+</sup>	2.030	4.4 · 10 <sup>4</sup>	Structure,[5] and rate.[6]
2	[Ni(H <sub>2</sub> O) <sub>6</sub> ] <sup>2+</sup>	2.030	3.2 · 10 <sup>4</sup>	Structure,[5] and rate.[7]
3	[Ni(H <sub>2</sub> O) <sub>2</sub> (NCS) <sub>4</sub> ] <sup>2-</sup>	2.071	1.1 · 10 <sup>6</sup>	Structure,[8] and rate.[9]
4	[Ni(H <sub>2</sub> O) <sub>3</sub> (NH <sub>3</sub> ) <sub>3</sub> ] <sup>2+</sup>	2.085	2.5 · 10 <sup>5</sup>	Structure,[10] and rate.[9]
5 <sup>b</sup>	[Ni(H <sub>2</sub> O) <sub>4</sub> (en)] <sup>2+</sup>	2.088	4.4 · 10 <sup>5</sup>	Structure,[11] and rate.[6]
6	[Ni(H <sub>2</sub> O) <sub>2</sub> (bipyridyl) <sub>2</sub> ] <sup>2+</sup>	2.090	6.6 · 10 <sup>4</sup>	Structure,[12] and rate.[9]
7	[Ni(H <sub>2</sub> O) <sub>5</sub> (NH <sub>3</sub> )] <sup>2+</sup>	2.104	1.6 · 10 <sup>5</sup>	Structure,[10] and rate.[13]

<sup>a</sup> Metal-to-oxygen distance. <sup>b</sup> en = ethylenediamine.

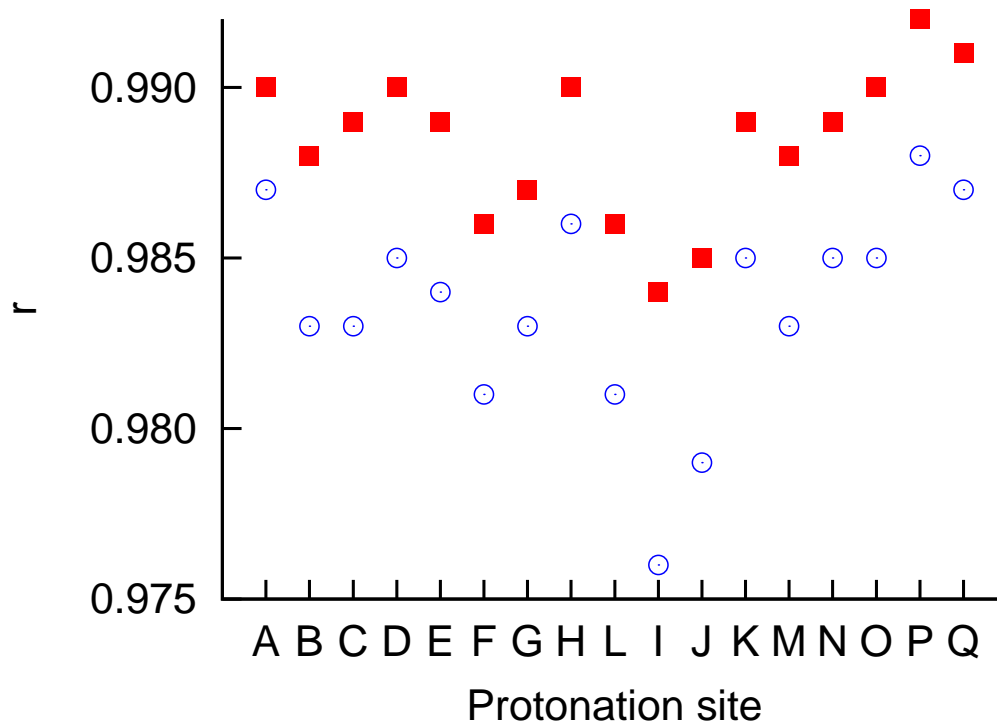
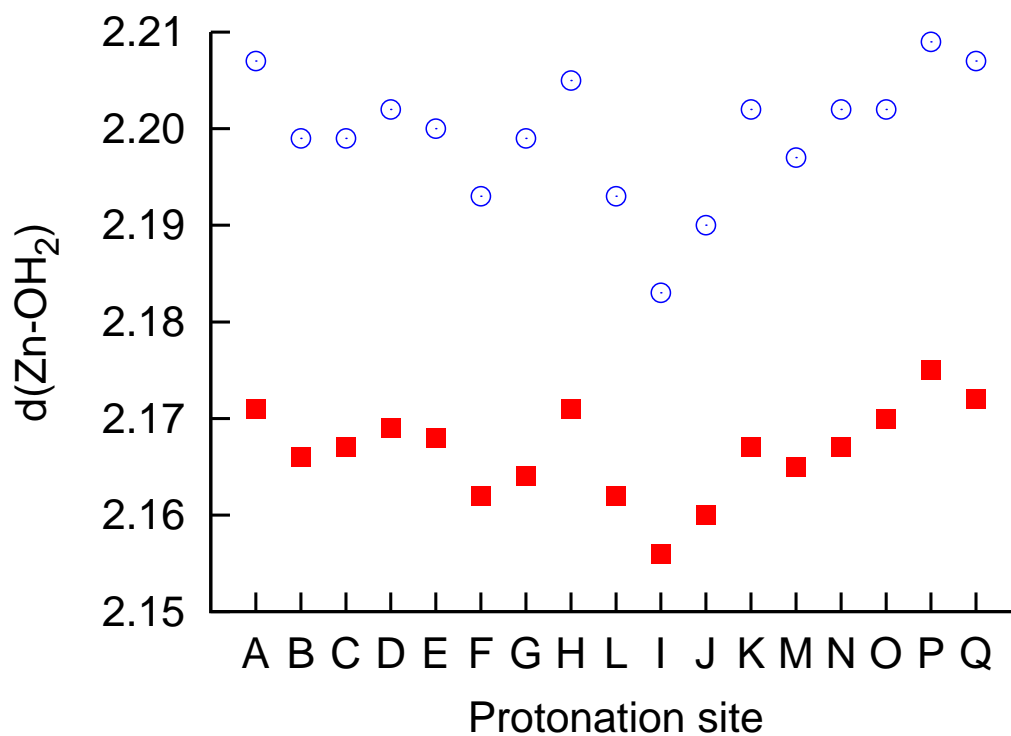


Figure S2: Top: Zn-OH<sub>2</sub> distance as a function of basis set. Bottom:  $r$  vs protonation site, where  $r$  is the Zn-OH<sub>2</sub> distance as a function of basis set divided by the Zn-OH<sub>2</sub> distance in the unprotonated complex at the same level of theory. Def2-svp results given as red squares and def2-tzvp data given as empty blue circles. The larger basis set gives longer absolute Zn-OH<sub>2</sub> distances, but also predicts a larger contraction due to protonation.

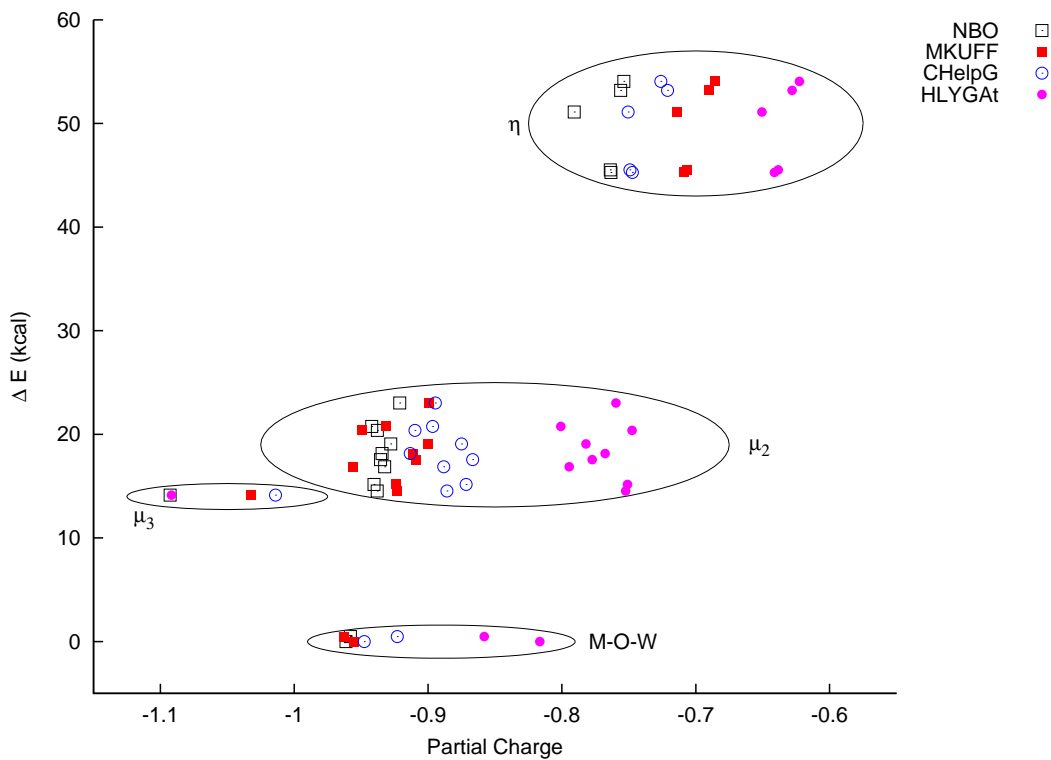


Figure S3: Comparison of partial charges from different methods at pbe0/def2-svp with relative energies of  $\text{H}_2[\text{Zn}_4(\text{H}_2\text{O})_2(\text{PW}_9\text{O}_{34})_2]^{8-}$  protonated in different loci. All partial charges methods indicate that site K ( $\mu_3$ ) has the most negative partial charge.



## References

- [1] E. D. Glendening, J. K. Badenhoop, A. E. Reed, J. E. Carpenter, J. A. Bohmann, C. M. Morales, C. R. Landis, F. Weinhold, *NBO 6.0*, <http://nbo6.chem.wisc.edu/>.
- [2] B. H. Besler, K. M. Merz, P. A. Kollman, *J. Comp. Chem.* **1990**, *11*, 431–439.
- [3] C. M. Breneman, K. B. Wiberg, *J. Comp. Chem.* **1990**, *11*, 361–373.
- [4] H. Hu, Z. Lu, W. Yang, *J. Chem. Theory Comp.* **2007**, *3*, 1004–1013, PMID: 26627419.
- [5] J. E. Morris, P. J. Squattrito, K. Kirschbaum, A. A. Pinkerton, *J. Chem. Cryst.* **2003**, *33*, 307–321.
- [6] A. G. Desai, H. W. Dodgen, J. P. Hunt, *J. Am. Chem. Soc.* **1969**, *91*, 5001–5004.
- [7] Y. Ducommun, K. E. Newman, A. E. Merbach, *Inorg. Chem.* **1980**, *19*, 3696–3703.
- [8] S. Sain, R. Saha, G. Pilet, D. Bandyopadhyay, *J. Mol. Struct.* **2010**, *984*, 350 – 353.
- [9] J. Hunt, *Coord. Chem. Rev.* **1971**, *7*, 1 – 10.
- [10] A. F. Benedetto, P. J. Squattrito, F. Adani, E. Montoneri, *Inorg. Chim. Acta* **1997**, *260*, 207 – 216.
- [11] G. J. McDougall, R. D. Hancock, *Dalton Trans.* **1980**, 654–658.
- [12] Y. Rodríguez-Martín, J. González-Platas, C. Ruiz-Pérez, *Acta Cryst. C* **1999**, *55*, 1087–1090.
- [13] S. Marks, H. W. Dodgen, J. P. Hunt, *Inorg. Chem.* **1968**, *7*, 836–837.